



ELSEVIER

Journal of Chromatography A, 910 (2001) 223–236

JOURNAL OF  
CHROMATOGRAPHY A

www.elsevier.com/locate/chroma

# Impact of the post-treatment conditions of parent silica on the silanization of *n*-octadecyl bonded silica packings in reversed-phase high-performance liquid chromatography

F. Großmann<sup>1</sup>, V. Ehwald<sup>2</sup>, C. du Fresne von Hohenesche\*, K.K. Unger

*Institut für Anorganische Chemie und Analytische Chemie, Duesbergweg 10–14, Johannes Gutenberg-Universität, 55128 Mainz, Germany*

Received 16 May 2000; received in revised form 16 October 2000; accepted 22 November 2000

## Abstract

Native mesoporous silica beads were subjected to a sequence of post-treatment procedure including hydrochloric acid treatment, calcination and subsequent rehydroxylation. The post-treated silica beads were converted into RP-18 silica by silanization with monochloro- and dimethoxy-*n*-octadecylsilanes, respectively. The influence of post-treatments and silanization conditions on the physico-chemical characteristics and on the chromatographic behaviour of the RP-silicas was studied. Also the changes of the pore structural parameters and the silanol group densities during the post-treatment and silanization were assessed. © 2001 Elsevier Science B.V. All rights reserved.

**Keywords:** Stationary phases, LC; Post-treatment procedures; Silanization; Silica, *n*-octadecyl bonded; Calcination; Rehydroxylation

## 1. Introduction

During the last decade, a new generation of reversed-phase (RP) packings have been introduced by column manufacturers which will replace the traditional RP packings developed in the 1980s. These packings are characterised by using highly purified and stabilised parent silicas and by employ-

ing improved methods of silanization [1]. In the context of this development, attempts have been made towards an improved chromatographic characterisation of RP columns in high-performance liquid chromatography (HPLC) using defined test procedures and analytes [2–4]. The aim of such tests is to elucidate the chromatographic properties of commercial RP columns in terms of hydrophobicity, silanophilic activity, polar retention and metal complexation. Based on these results, chemometric approaches were used for a rational comparison, grouping and ranking of RP columns. Such tests are only meaningful when the retention, peak symmetry and selectivity of the test analytes truly reflect the stationary phase properties through understandable chromatographic retention processes. In other words,

\*Corresponding author. Tel.: +49-6131-392-5745; fax: +49-6131-392-2710.

*E-mail address:* unger@ak-unger.chemie.uni-mainz.de (C. du Fresne von Hohenesche).

<sup>1</sup>Present address: SÜD-Chemie AG, 80333 Munich, Germany.

<sup>2</sup>Present address: Wacker Chemie GmbH, 84489 Burghausen, Germany.

the results should not be affected by stationary phase impurities, mutual interferences of analytes in the test mixture, overloading effects, etc. One of the most critical steps in the manufacture of the RP packings is the post-treatment of the native silica prior to silanization. The term post-treatment collectively stands for a number of processes such as treatment with acids, bases, complexation reagents, hydrothermal and thermal procedures, respectively, resulting in higher purity and stability of the silica packing. A limited number of studies have been reported in this field, mainly performed on traditional but not high-purity silicas [5–8]. The objective of this study is to subject a high-purity silica to various extraction, dehydroxylation and rehydroxylation processes prior to silanization with *n*-octadecyldimethylmonochlorosilane and *n*-octadecylmethyl-dimethoxysilane, respectively, and to elucidate the impact of the post-treatment procedures, as well as their conditions on the chromatographic properties, using standard test mixtures for the characterisation of the prepared RP 18 HPLC columns.

## 2. Experimental

### 2.1. Native porous silica

The silica was prepared by hydrolysis and condensation of a partially condensed tetraethoxysilane (TES40; Wacker, Burghausen, Germany) in a two-step procedure described elsewhere [9]. The first step comprised the hydrolysis and condensation to a polyethoxysiloxane (PES) with a molecular mass of approximately 1000 g/mol. The purified PES was then converted in an emulsion under rigorous stirring to silica hydrogel beads. The beads were subjected to sedimentation to remove the fines and then dried at 150°C for 12 h.

### 2.2. Post-treatment

The batch was size-classified into a narrow fraction of an average particle diameter of  $d_p = 6 \mu\text{m}$  using a zig-zag sieve 100 MZR (Alpine, Augsburg, Germany). The sized batch was subjected to a treatment with hydrochloric acid (reagent grade) of 37% (w/w) for 20 h to remove metal impurities

which were introduced by the sizing process. The extracted material was calcined in a shallow bed in a furnace (N 100; Nabertherm, Lilienthal, Germany) in the range between 550 and 1000°C for a period of 5 h with a heating rate of 1 K/min. The rehydroxylation was performed by refluxing the calcined sample with hydrochloric acid (17%, w/w) for a period of 2 and 20 h, respectively.

### 2.3. Calcium hydroxide treatment

A 1-g amount of calcium hydroxide (analytical-reagent grade; Merck, Darmstadt, Germany) was dissolved in 100 ml of deionised water in a 250-ml round bottom flask. The solution was filtered after 20 min. The pH of a suspension of 5 g of post-treated silica and 60 ml deionised water was adjusted with the  $\text{Ca}(\text{OH})_2$  solution to pH 7 (in a second experiment: pH 9). After boiling, with stirring, for 2 min, the suspension was filtered and washed with 2 l of deionised water and 50 ml of methanol.

### 2.4. Reversed-phase silica

#### 2.4.1. Silanisation procedure A

A 100-g amount of rehydroxylated silica (dried at 150°C and 12 hPa for 12 h) was poured into an evacuated and nitrogen-flushed, 1000-ml, three-neck round-bottom flask, equipped with a Dimroth-condenser, a stirrer bearing, a stirring shaft and a stirring motor. A 400-ml volume of dry *N,N*-dimethylformamide (analytical-reagent grade; Merck) was added under stirring. Subsequently a solution of 24.97 g *N*-methyl-2-pyrrolidinone (analytical-reagent grade; Merck) in 200 ml *N,N*-dimethylformamide was prepared and 72.89 g of melted *n*-octadecyldimethylchlorosilane (Wacker) was added to that solution. This whole solution was added within 20 min to the silica suspension, under nitrogen and stirring. The flask was sunk into a preheated oil-bath and the suspension was heated for 2 h, at a temperature of 120°C. After cooling for 30 min, the suspension was filtered through a glass filter funnel. The silanised silica was sequentially washed with 300 ml of *N,N*-dimethylformamide, 300 ml of methanol (analytical-reagent grade; Merck), 300 ml of methanol–water (50:50, v/v) and finally with 300 ml of methanol. The residue was consequently subjected to tetrahy-

drofuran (THF)-treatment by pouring it into a 1000-ml, three-neck round-bottom flask, equipped with a Dimroth-condenser, a stirrer bearing, a stirring shaft and a stirring motor. A 500-ml volume of THF (analytical-reagent grade; Merck) was added and the suspension was refluxed, with stirring, for 20 min. After removal of the oil-bath the suspension was immediately filtered through a glass filter funnel and washed with 300 ml tetrahydrofuran and twice with 300 ml of methanol. Finally, the product was dried at 40°C, for 12 h at a pressure of 12 hPa.

#### 2.4.2. Silanisation procedure B

A 100-g amount of silica (dried at 150°C and 12 hPa for 4 h) was wetted in a 1-l three-neck round-bottom flask with 5.63 ml of deionized water using a transfer pipette. The wetted silica was shaken and allowed to stand for 12 h. After 12 h, a 1000-ml three-neck round-bottom flask equipped with a Dimroth-condenser, a stirrer-bearing, a stirring-shaft and a stirring motor, was evacuated and flushed with nitrogen. A 400-ml volume of toluene (analytical-reagent grade; Merck) was added to the silica under nitrogen, while stirring. A 19.62-ml volume of an 80 g *p*-toluenesulfonic acid (analytical-reagent grade; Merck) solution in 1 l of dimethylformamide, and 75.33 g of *n*-octadecylmethyldimethoxysilane (Wacker) were mixed in 350 ml of toluene and added immediately to the stirred silica under nitrogen. The flask was sunk into a preheated oil-bath held at 150°C and the suspension refluxed under stirring for 2 h. The suspension was then allowed to cool for 30 min. Afterwards the silica was filtered through a glass filter funnel and sequentially washed with 300 ml each of toluene, methanol, methanol–water (50:50, v/v) and finally with 300 ml of methanol. The residue was subjected to THF-treatment as mentioned in silanization procedure A.

#### 2.5. Physico–chemical characterisation

Size analysis of sized native silica beads was performed using a Coulter Counter Multisizer Accu-Comp 1.19 (Merck). Thermal analysis was conducted with a thermobalance under room atmosphere and pressure (Model L 81; Linseis, Selb, Germany). The heating rate for all analyses was 10°C/min up to 1000°C. After activation at 423 K and 20 hPa for 12

h, the specific surface area according to BET was determined by nitrogen sorption at 77 K using an Autosorb 6 (Quantachrome, USA). The concentration of surface hydroxyl groups ( $\alpha_{\text{OH}}$ ) was determined by means of isotopic exchange with deuterated trifluoroacetic acid followed by  $^1\text{H}$ -nuclear magnetic resonance (NMR) spectroscopy according to the method of Holik and Matějková [10]. A detailed description of the method can be found in Refs. [11,12]. In comparison to this method the silanol group concentration was also calculated via the mass loss between 200 and 1000°C measured by thermal gravimetry [12]. The carbon content was measured by elemental analysis (CHN-rapid; Heraeus, Hanau, Germany). The *n*-octadecyl ligand density,  $\alpha_{\text{C}_{18}}$ , was calculated from the carbon content of the modified silicas, using the specific surface area according to the formula [13] shown in Eq. (1):

$$\alpha_{\text{exp}} = \frac{P_{\text{C}} \cdot 10^6}{1200 \cdot n_{\text{C}} - P_{\text{C}} \cdot (M - n_{\text{x}})} \cdot \frac{1}{a_{\text{s}}} \quad (1)$$

where  $\alpha_{\text{exp}}$  is the ligand density [ $\mu\text{mol}/\text{m}^2$ ],  $P_{\text{C}}$  is the carbon content [%C, w/w],  $n_{\text{C}}$  is the number of C atoms in the bonded silane,  $M$  is the molecular mass of the silane,  $n_{\text{x}}$  is the number of functional groups of the silane and  $a_{\text{s}}$  is the specific surface area (BET) [ $\text{m}^2/\text{g}$ ].

#### 2.6. Chromatographic measurements

The reversed-phase silica was packed into  $150 \times 4.0$  mm I.D. columns by the slurry technique. Analyses were performed using an analytical dual piston pump (Model 2250; Bischoff Analysentechnik und Gerätebau, Leonberg, Germany), an oven (PYE UNICAM PU 4031; Philips, Eindhoven, The Netherlands) and a UV detector (Lambda UV 1000; Bischoff Analysentechnik und Gerätebau). All eluents used were of HPLC grade. Water was purified by means of a Millipore Milli-Q 185 Plus (Millipore, Watford, UK). Data acquisition and integration was controlled by a normal personal computer using standard software (Hyperdata Chromsoft, Version 2.06; Autochrom, USA). To assess the silanophilic properties and the metal activity of the stationary phases, three different test mixtures were applied at a column temperature of  $40 \pm 0.1^\circ\text{C}$ .

### 2.6.1. Test mixture 1: silanophilic activity according to Engelhardt–Jungheim

A mobile phase containing water–methanol (51:49, v/v) was employed [14]. A 10- $\mu$ l volume of the test solution, which contained uracil (0.1 g/l), aniline (1.0 g/l), phenol (1.0 g/l), *p*-ethylaniline (1.0 g/l) and *N,N*-dimethylaniline (0.2 g/l) was injected. The silanophilic property of the stationary phase was expressed as the separation factor of aniline and phenol. Additionally, as recently proposed by Engelhardt [15], the silanophilic property of the stationary phase was evaluated on the peak symmetry of *p*-ethylaniline in an unbuffered mobile phase. The peak symmetry was calculated as the “asymmetry factor” ( $b/a$ ) at 10% of the peak height [16].

### 2.6.2. Test mixture 2: silanophilic activity tested with pyridine and phenol

A mobile phase containing water–acetonitrile (70:30, v/v) was employed. A 10- $\mu$ l volume of the test solution, which contained thiourea (0.025 g/l), pyridine (0.020 g/l) and phenol (0.075 g/l) was injected. This test mixture is used by several column manufacturers as a standard test mixture to assess the chromatographic performance of the stationary phases. The peak symmetry and elution order of pyridine and phenol was taken as a measure for the silanophilic activity of the stationary phase [17]. The  $pK_b$  value of pyridine ( $pK_b$  8.8) compared to aniline ( $pK_b$  9.38) recommends pyridine as a trace molecule for silanophilic activity of a stationary phase. In water-containing eluents pyridine interacts via hydrophobic interactions as well as by ionic exchange mechanisms with the silica surface. The hydrophobicity of pyridine, given as the partition coefficient in

*n*-octanol–water [18] is smaller ( $\log P=0.64$ ) compared to phenol ( $\log P=1.46$ ). Therefore it is usually agreed that, on stationary phases with a low silanophilic activity, pyridine is eluted before phenol.

### 2.6.3. Test mixture 3: metal activity test with 2,2'-bipyridyl and 4,4'-bipyridyl

Test mixture 3 (1.0 g/l 2,2'-bipyridyl and 0.25 g/l 4,4'-bipyridyl) was used with a mobile phase containing water–methanol (51:49, v/v). The elution behaviour of 2,2'- and 4,4'-bipyridyl in dependence of the metal content of a stationary phase is presently under investigation [19,20,14]. The retention factor and peak area of 2,2'-bipyridyl, as a metal complexing molecule, is strongly dependent on the metal concentration on the surface of the stationary phase. 4,4'-Bipyridyl is interesting as a trace solute for the silanophilic activity of the stationary phase. The peak tailing and retention time of 2,2'-bipyridyl and 4,4'-bipyridyl was taken as a measure of the metal content. The effect of metal accumulation on column heads during use (metal contamination from solvent frits, etc.) was minimised by testing all the columns under investigation in the same test sequence.

## 3. Results and discussion

### 3.1. Dependence of the pore structural parameters on the post-treatment

#### 3.1.1. Metal content

A batch of native silica was sized in a 6- $\mu$ m fraction with the following particle size distribution:  $d_{p90}=7.8$   $\mu$ m,  $d_{p50}=6.0$   $\mu$ m,  $d_{p10}=4.3$   $\mu$ m. Aliquots of the silica were subjected to a treatment

Table 1  
Metal content of the silica batch before and after the treatment with hydrochloric acid

Element	Unsize silica (ppm)	Sized silica (ppm)	After 2 h HCl treatment (ppm)	After 20 h HCl treatment (ppm)
Fe	<1	50	6	<1
Ni	<1	4	<1	<1
Zn	<1	2	<1	<1
Cu	<1	<1	<1	<1
Pb	<1	<1	<1	<1
Co	<1	<1	<1	<1
Al	<1	<1	<1	<1

with conc. hydrochloric acid as described in the Experimental section. Table 1 shows the results of the metal analysis before and after extraction. There is a notable increase in the iron content of the silica after sizing. Extensive treatment with concentrated hydrochloric acid afterwards reduced the content to <1 ppm. Other metals have been below the 1 ppm level.

### 3.1.2. Dehydroxylation – rehydroxylation procedure

Calcination of porous silicas in the temperature range between 200 and 1000°C is well investigated and monitored by various physico–chemical methods [21–24]. Annealing a mesoporous silica above 100°C leads to the removal of physisorbed water, which is completed between 150 and 200°C. Above 150°C the condensation of vicinal hydroxyl groups starts, leaving strained siloxane groups. Up to about 500–600°C this process is nearly completed. The condensation is accompanied by a change in the pore structure of the silica. Both the specific surface area and the specific pore volume decrease and the pore structure start to collapse. The temperature range where sintering occurs varies from silica to silica and strongly depends on the content of metal impurities, e.g., the sodium content. In other words, highly pure silicas are much more stable than those containing sodium at a concentration in excess of 100 ppm [25]. The rehydroxylation of silicas which have been calcined above 600°C is a slow process. The rehydroxylation reaction is shown in Fig. 1 [26,27]. Table 2 shows the data of the specific surface area,  $a_s$  (BET), the specific pore volume,  $v_p$  (G), and the average pore diameter,  $p_d$  (BJH), as a function of the calcination temperature ranging from 550 to 1000°C before and after rehydroxylation. It can be clearly

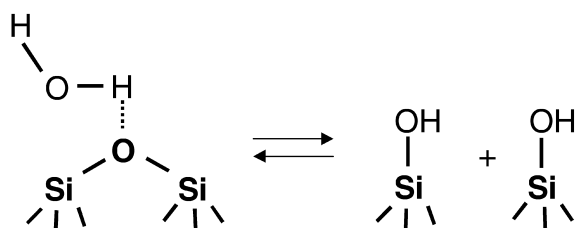


Fig. 1. Rehydroxylation of siloxane groups.

seen that the surface is passing through an activation process. The increase of surface area can be explained by the burn off of unreacted ethoxy groups causing the formation of new pores or the opening of internal pores. Sintering occurs at a temperature above 700°C and the values of  $a_s$  (BET),  $v_p$  (G) and  $p_d$  (BJH) fall drastically. In these cases the average pore diameter showed to be more sensitive to this process than the specific surface area. However, even after calcination at 1000°C the silica possesses a substantial porosity and specific surface area but behaves completely hydrophobically.

### 3.1.3. Reproducibility and apparent density

In order to assess the changes of the pore structural parameters as a function of the calcination temperature, the operational parameters controlling the reproducibility were studied (data not shown). It was found that following conditions have to be maintained:

- (i) A defined shallow bed calcination is mandatory to assess the reproducibility of the calcination process.
- (ii) The heating rate must be controlled and should be monitored.
- (iii) The hold up temperature must be adjusted within  $\pm 5^\circ\text{C}$ .

Table 2

Changes of the specific surface area,  $a_s$  (BET), the specific pore volume,  $v_p$  (G), and the pore diameter,  $p_d$  (BJH), with the calcination temperature and after rehydroxylation (rehydr.) of calcined samples<sup>a</sup>

Parameter	Calcination temperature (°C)															
	Native	550	Rehydr.	650	Rehydr.	700	Rehydr.	Native	750	Rehydr.	800	Rehydr.	900	Rehydr.	1000	Rehydr.
$a_s$ (BET) (m <sup>2</sup> /g)	347	+12.4	-1.2	+13.4	-0.7	-0.3	-5.0	341	+1.0	-4.5	-5.9	-10.0	-12.9	-10.3	-27.9	-29.7
$v_p$ (ml/g)	1.12	+2.7	-2.6	-1.5	-4.7	-0.9	-4.9	1.21	-8.5	-10.8	-9.9	-12.0	-18.4	-17.7	-42.4	-44.3
$p_d$ (BJH) (Å)	113.7	+0.3	+0.8	-0.3	+0.7	0	-2.6	118	+0.7	+1.7	0	-6.0	-3.5	-10.2	-23.7	-23.8

<sup>a</sup> Changes are given in % related to the value of the parent silica.

The reproducibility of the pore structural parameters was in the range of  $\pm 0.1$ – $0.3\%$ .

Calcination and rehydroxylation are essential tools to adjust the pore structural parameters. The post-treatment is expected to densify and stabilise the bulk structure and to heal inhomogeneities in the surface. Monitoring the apparent density according to helium indicates that  $\rho_{\text{app(He)}}$  increases from 2.20 g/ml of the native silica to 2.50 g/ml of the calcined silica at 600, 700 and 800°C, respectively. By rehydroxylation,  $\rho_{\text{app(He)}}$  decreases to about 2.25 g/ml for all treated silicas. Thus, the effect of densification is not as pronounced as expected.

### 3.1.4. Silanol group densities

The measurements of  $\alpha_{\text{OH}}$  by deuterium exchange with  $\text{CF}_3\text{COOD}$  followed by  $^1\text{H-NMR}$  spectroscopy are compared with those obtained by thermal analysis and are presented in Fig. 2. The parent silica had an  $\alpha_{\text{OH}}$  value of  $9.5 \mu\text{mol}/\text{m}^2$  which is a little higher than the average value for a fully hydroxylated surface ( $8.2 \pm 1.0 \mu\text{mol}/\text{m}^2$ ) [21]. The calcination at various temperatures lead to a decrease of  $\alpha_{\text{OH}}$ . Both methods are able to show the expected decrease of  $\alpha_{\text{OH}}$  with increasing calcination temperature and are consistent with the measurements of  $\alpha_{\text{OH}}$  by cross-polarization magic angle spinning  $^{29}\text{Si}$ -nuclear magnetic resonance ( $^{29}\text{Si-CP-MAS-NMR}$ ) (not shown here). The subsequent rehydroxylation enhances  $\alpha_{\text{OH}}$  but the higher the applied calcination temperature the less the completion of rehydroxylation. The process

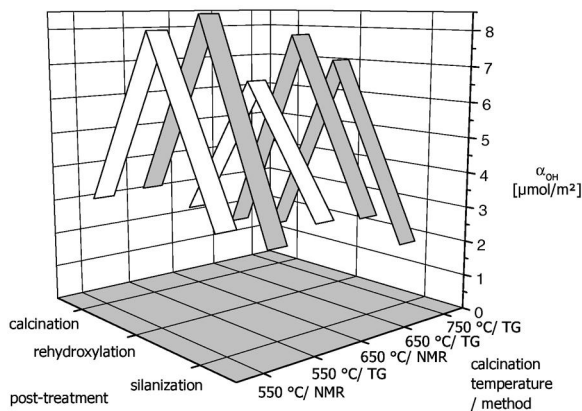


Fig. 2. Silanol group densities of silica samples subjected to post-treatments starting with calcination at different temperatures.

seemed not to be fully reversible which can be explained by the formation of strained siloxane bonds during the condensation process. Those bondings are converted to more stable siloxane groups at high temperatures. The conversion is too slow and the initial value is not reached. Despite of the different silanol group densities for the rehydroxylated silicas, silanisation lead to nearly the same *n*-alkyl ligand densities in all cases. This suggests that reactive silanol species are not affected by the applied post-treatments.

### 3.2. Dependence of the ligand density on the calcination and silanization

To evaluate the impact of the dehydroxylation – rehydroxylation conditions on the ligand densities of *n*-octadecyl groups, the native silica was thermally treated at 600, 700, 800 and 1000°C, respectively. All samples were then rehydroxylated with a hydrochloric acid solution of 17% (w/w) for 3 h. The samples were silanized following two procedures, A and B (see Experimental section). The results are shown in Fig. 3. The ligand densities in both cases were not affected by the thermal treatment of the parent silica, although the carbon content decreased. This can be explained with the decrease of the specific surface area (see Table 2) due to the sintering process.

### 3.3. Maximising the *n*-octadecyl ligand density $\alpha_{\text{C}_{18}}$

In order to increase the ligand density, the reaction of silica with *n*-octadecyldimethylmonochlorosilane was carried out with imidazole as catalyst and toluene as solvent [28]. Under these conditions a ligand density of  $3.2 \mu\text{mol}/\text{m}^2$  was achieved, which was substantially higher than those obtained by the other procedures. A second silanization with hexamethyldichlorosilazane (HMDS) was performed to elucidate the effect of endcapping on  $\alpha_{\text{C}_{18}}$ . Table 3 collects the results. They reveal that  $\alpha_{\text{C}_{18}}$  only increases with the two  $\text{C}_{18}$  bonded silicas with the lower ligand densities. Endcapping has scarcely any effect on the  $\text{C}_{18}$  bonded silica prepared with imidazole as a catalyst [29].

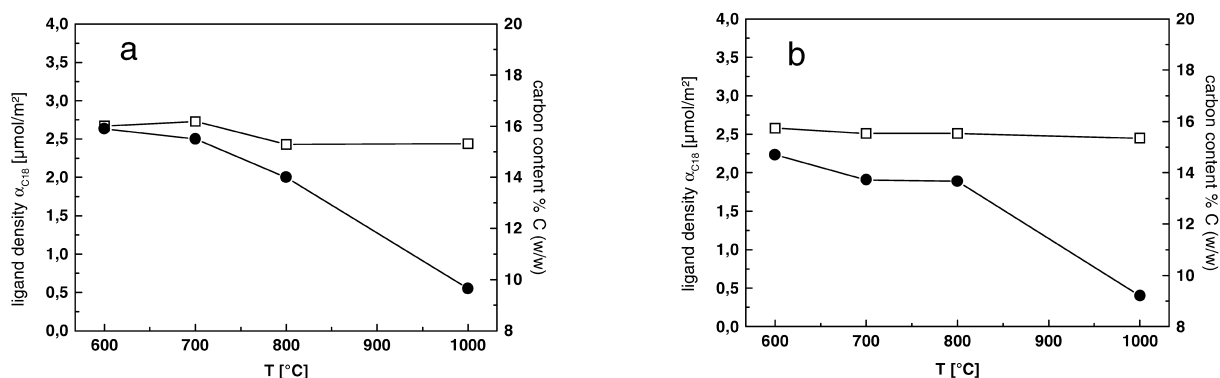


Fig. 3. Carbon content (●) and *n*-octadecylsilyl ligand density  $\alpha_{C_{18}}$  (□) as a function of the calcination temperature of the parent silica. (a) Silanization with *n*-octadecyldimethylchlorosilane; (b) silanization with *n*-octadecylmethyldimethoxysilane.

### 3.4. Chromatographic results

#### 3.4.1. Results for test mixture 1

##### 3.4.1.1. *n*-Octadecyldimethylchlorosilane modified silicas

A series of different *n*-octadecyldimethylchlorosilane modified RP silicas were tested with test mixture 1 (see Fig. 4, chromatograms 1–5). RP-18 silica KGS1 (see Table 4), with a rather low  $C_{18}$  ligand density of 2.65  $\mu\text{mol}/\text{m}^2$ , does not separate aniline and phenol (No.1). The analytes are coeluting. HCl treatment of the parent silica prior to silanization improves the peak symmetry of *p*-ethylaniline from 5.61 to 1.54 (No. 2). The peak symmetry is comparable to that of a commercially available  $C_{18}$  column. The ability to separate aniline and phenol is not affected by the reduction of the metal induced silanophilic activity of the stationary phase minimised by HCl treatment of the parent silica. Endcapping of packing KGS3 leads to packing KGS5, with a total ligand density  $\alpha_{\text{exp}}$  ( $\alpha_{C_{18}} + \alpha_{C_1}$ )

of 3.05  $\mu\text{mol}/\text{m}^2$ . This stationary phase shows a baseline separation of aniline and phenol (No. 3). The peak symmetry of *p*-ethylaniline is not affected by endcapping. The silica KGS7 with a higher amount of bonding is able to resolve aniline and phenol and *p*-ethylaniline elutes with a good peak shape. Endcapping of this densely  $C_{18}$  bonded material does not have any effect. This behaviour shows, the silanol groups, which are still present after a first silanization, to be responsible for the ability of a  $C_{18}$  phase to separate aniline and phenol. The lower their concentration, the better the aniline/phenol separation. These silanol groups are not responsible for the peak shape of *p*-ethylaniline, which depends on the metal induced activity of silanol groups on the silica surface.

##### 3.4.1.2. *n*-Octadecylmethyldimethoxysilane modified silicas

Another series of three different *n*-octadecylmethyldimethoxysilane modified RP silicas was also tested with test mixture 1 (see Fig. 5, chromatograms 6–8). Silicas silanized with *n*-octa-

Table 3  
Changes of the carbon content of silanized silicas after treatment with HMDS

Silica	Silane	Solvent/ catalyst	%C, $C_{18}$ (w/w)	$\alpha_{C_{18}}$ ( $\mu\text{mol}/\text{m}^2$ )	%C, HMDS (w/w)	$\alpha_{\text{total}}$ ( $\mu\text{mol}/\text{m}^2$ )
UM4	$\text{ClSi}(\text{CH}_3)_2\text{C}_{18}\text{H}_{37}$	DMF/NMP	15.70	2.65	16.30	3.18
UM4	$\text{ClSi}(\text{CH}_3)_2\text{C}_{18}\text{H}_{37}$	Toluene/imidazole	17.78	3.10	17.84	3.15
UM4	$(\text{CH}_3\text{O})_2\text{Si}(\text{CH}_3)\text{C}_{18}\text{H}_{37}$	Toluene/PTS	13.00	2.20	13.75	3.38

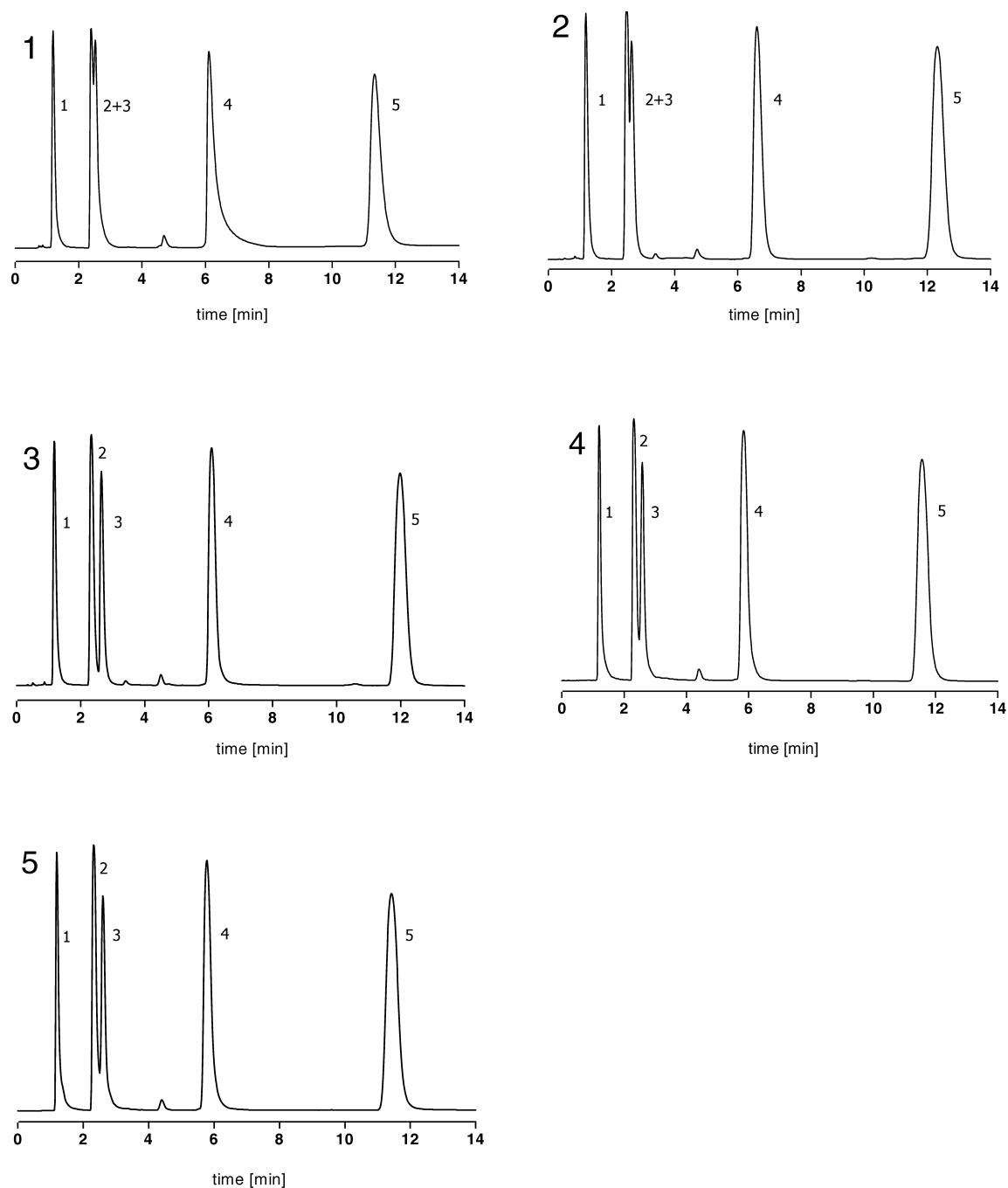


Fig. 4. Chromatograms 1–5: elution of modified Engelhard test mixture on *n*-octadecyldimethylchlorosilane modified silicas. Peaks in order of elution: 1=uracil, 2=aniline, 3=phenol (chromatogram Nos. 1 and 2, coelution of aniline and phenol), 4=*p*-ethylaniline, 5=*N,N*-dimethylaniline. Eluent: water–MeOH (51:49, v/v), column temperature 40°C, flow 1.0 ml/min, detection at 254 nm.



Table 4

RP silica Nos. 1–5 – post-treatment parameters, ligand density  $\alpha_{\text{exp}}$ , retention factors and peak symmetry of *p*-ethylaniline

No.	Silica	HCl treatment	Endcapping	$\alpha_{\text{exp}}$ ( $\mu\text{mol}/\text{m}^2$ )	<i>p</i> -Ethylaniline	
					<i>k</i>	PS
1	KGS1	–	–	2.65	4.08	5.61
2	KGS3	20 h	–	2.69	4.52	1.54
3	KGS5	20 h	Of KGS3	3.05	4.12	1.62
4	KGS7	20 h	–	3.12	3.70	1.69
5	KGS8	20 h	Of KGS7	3.22	3.79	1.72

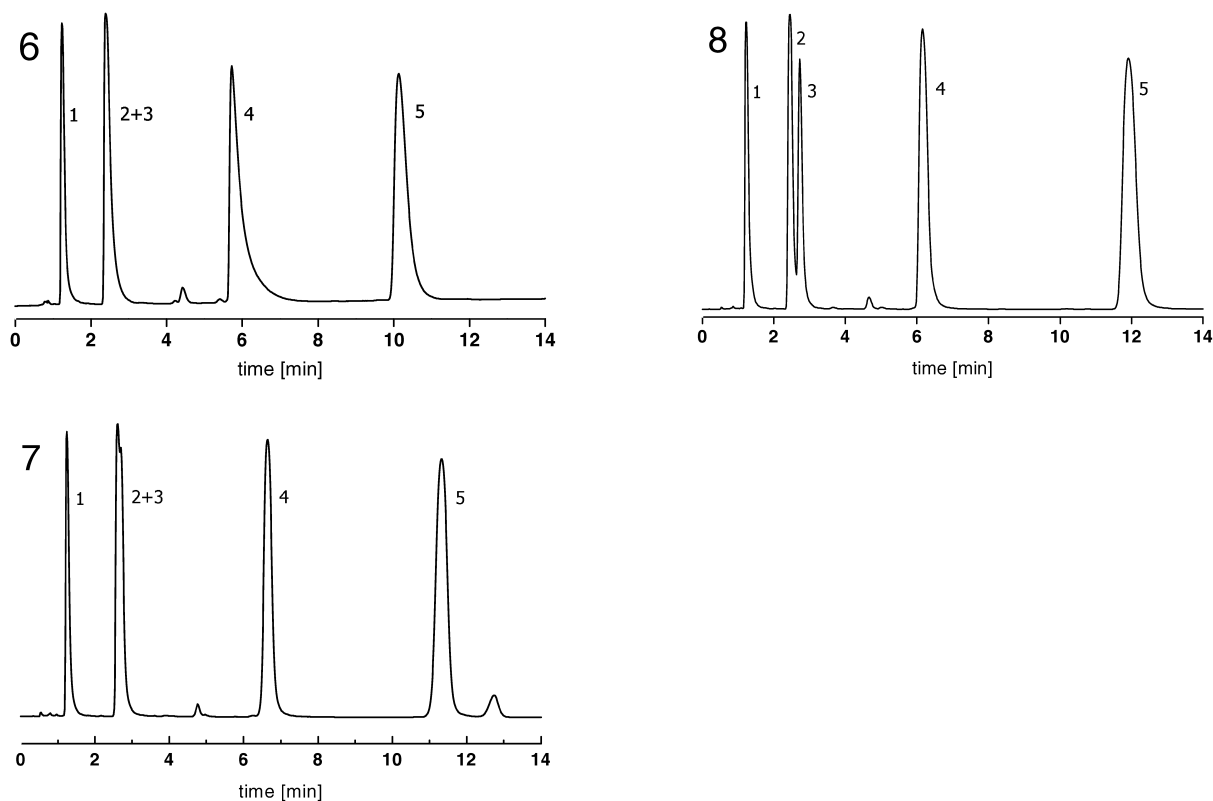


Fig. 5. Chromatograms 6–8: modified Engelhard test mixture on *n*-octadecylmethyldimethoxysilane modified silicas. Peaks in order of elution: 1 = uracil, 2 = aniline, 3 = phenol, 4 = *p*-ethylaniline, 5 = *N,N*-dimethylaniline. Eluent: water–MeOH (51:49, v/v), column temperature 40°C, flow 1.0 ml/min, detection at 254 nm.

Table 5

Physical parameters of RP silica Nos. 6–8 – HCl treatment of parent silicas, ligand density  $\alpha_{\text{exp}}$ , retention factors and peak symmetry of *p*-ethylaniline

No.	Silica	HCl treatment	Endcapping	$\alpha_{\text{exp}}$ ( $\mu\text{mol}/\text{m}^2$ )	<i>p</i> -Ethylaniline	
					<i>k</i>	PS
6	KGS2	–	–	2.61	3.58	5.91
7	KGS4	20 h	–	2.25	4.29	1.23
8	KGS6	20 h	Of KGS4	2.89	3.97	1.65

decylmethyldimethoxysilane showed the same chromatographic behaviour as the chlorosilane modified silicas, at a lower total ligand density. Acid treatment of the parent silica improved the peak profile of *p*-ethylaniline but did not improve the separation of aniline and phenol. Only endcapping of the bonded phases increased the  $\alpha$  value between aniline and phenol (see Table 5). As shown for the *n*-octadecyldimethylchlorosilane modified silicas this texture allows the separation of the chromatographic effects of metal induced strong acid sites and overall silanol activity caused by remaining silanol groups on the silica surface.

### 3.4.2. Results of the test mixture 2 – *n*-octadecyldimethylchlorosilane modified silicas

Chromatogram No. 9 in Fig. 6 shows an elution of phenol and pyridine which is expected from a stationary phase with a high silanophilic activity [17]. Pyridine elutes after phenol with a poor peak symmetry. When the same parent silica was treated with hydrochloric acid prior to silanization at comparable ligand density, the retention factor of pyridine decreased together with an improved peak symmetry (No. 10). When this RP-silica is endcapped, pyridine elutes in front of phenol with a good peak shape which one normally expects for a commercial RP-18 column (No. 11). The higher bonded acid treated parent silica elutes pyridine in front of phenol (No. 12). With the endcapped higher bonded silica pyridine elutes earlier at comparable peak symmetry (Nos. 13 and 14). Endcapping is more effective with regard to peak symmetry and the retention factor of pyridine for silicas with lower  $C_{18}$

surface concentration (see Table 6). A good chromatogram was obtained with silica KGS10. This parent silica was treated before silanization with a dilute solution of  $\text{Ca}(\text{OH})_2$  (pH 9). As shown in chromatogram No. 15, pyridine is eluted before phenol with good peak shape. This silanized silica was not endcapped. The alkaline treatment of the silica and the deposition of calcium ions obviously reduced the acidic nature of the silanol groups and generated a homogeneous silica surface. This effect was more pronounced if the silica was treated at a pH of 9 compared to a pH of 7.

### 3.4.3. Results of the test mixture 3 – *n*-octadecyldimethylchlorosilane modified silicas

The chromatogram Nos. 16–20 (see Fig. 7) were obtained with *n*-octadecyldimethylchlorosilane modified silicas and test mixture 3. Chromatogram Nos. 16 and 17 show the influence of the HCl treatment on the elution of 2,2'-bipyridine. The silica without HCl treatment (KGS1, see Table 7) contains a high concentration of metals on the silica surface. Therefore 2,2'-bipyridine showed high interaction with the silica surface, resulting in strong chromatographic peak tailing. Reduction of the metal concentration improved the peak shape of 2,2'-bipyridine and reduced the retention time, as it is shown in chromatogram No. 17. The retention time or peak shape of the 4,4' isomer is not affected by the HCl treatment. Endcapping of this silica again reduced the retention time of both isomers (elution order: 4,4' isomer before the 2,2' isomer, as observed for commercial silica columns) and improved the peak shape (No. 18). The retention time and peak shape of

Table 6

Physical parameters of RP silica Nos. 9–15 – HCl treatment of parent silicas, total ligand density  $\alpha_{\text{exp}}$ , retention factors for pyridine and phenol, separation factor between pyridine and phenol and peak symmetry for pyridine

No.	Silica	Treatment	Endcapping	$\alpha_{\text{exp}}$ ( $\mu\text{mol}/\text{m}^2$ )	$k$		$\alpha_{\text{py/ph}}$	PS (pyridine)
					Pyridine	Phenol		
9	KGS 1	–	–	2.65	2.75	1.99	1.38	2.46
10	KGS 3	20 h HCl	–	2.69	2.31	2.13	1.08	1.89
11	KGS 5	20 h HCl	Of KGS3	3.05	1.52	2.10	0.72	1.95
12	KGS 7	20 h HCl	–	3.12	1.89	2.10	0.90	2.18
13	KGS 8	20 h HCl	Of KGS7	3.22	1.73	2.10	0.82	2.24
14	KGS 9	20 h HCl + $\text{Ca}(\text{OH})_2$ , pH 7	–	3.09	1.65	2.04	0.81	2.04
15	KGS 10	20 h HCl + $\text{Ca}(\text{OH})_2$ , pH 9	–	3.22	1.35	1.96	0.69	1.55

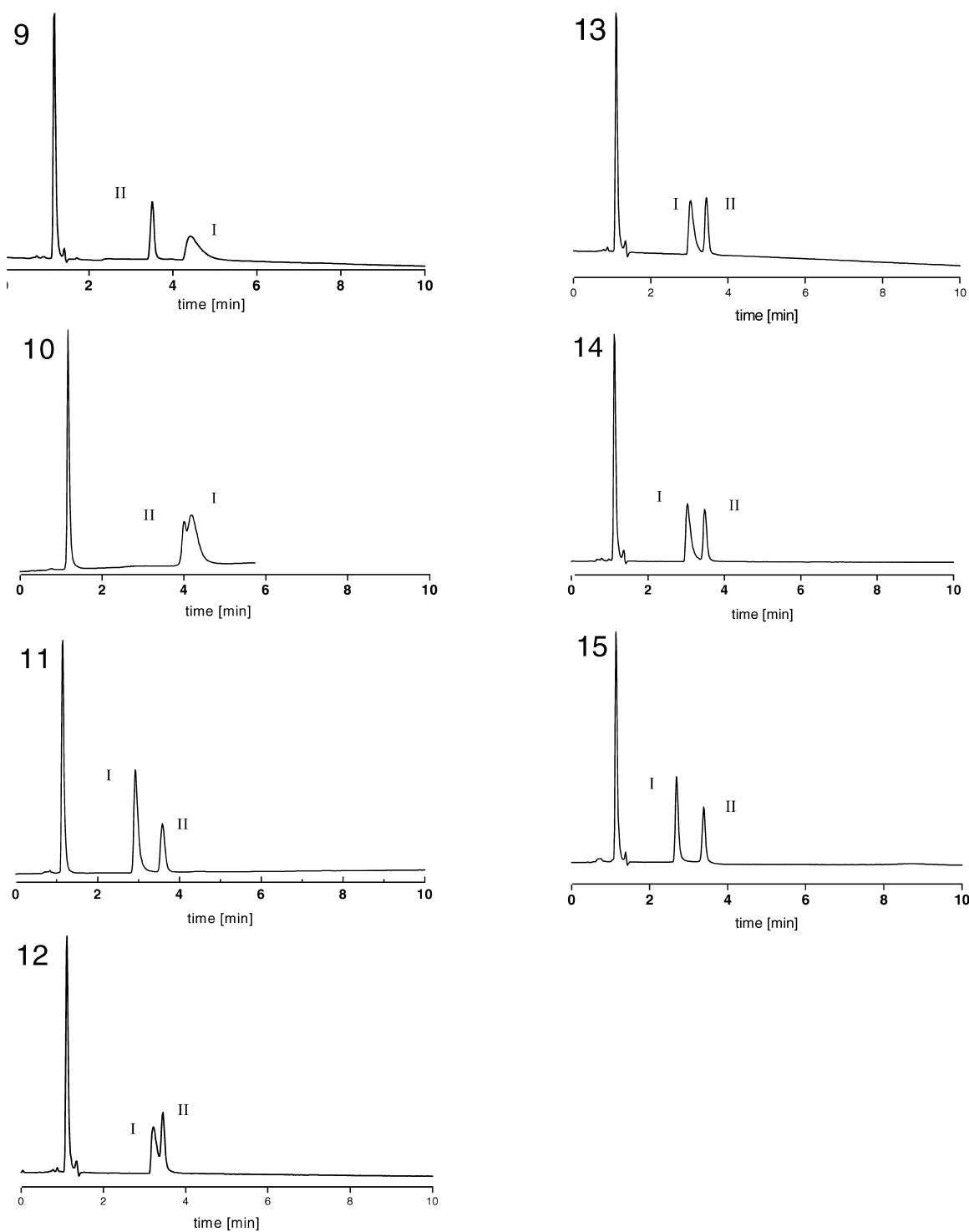


Fig. 6. Chromatograms 9–15: pyridine–phenol test mixture (test mixture II). Peaks: 1=thiourea, 2=pyridine, 3=phenol. Eluent: water–CH<sub>3</sub>CN (70:30, v/v), column temperature 40°C, flow 1.0 ml/min, detection at 254 nm. Peak I=pyridine; Peak II=phenol.

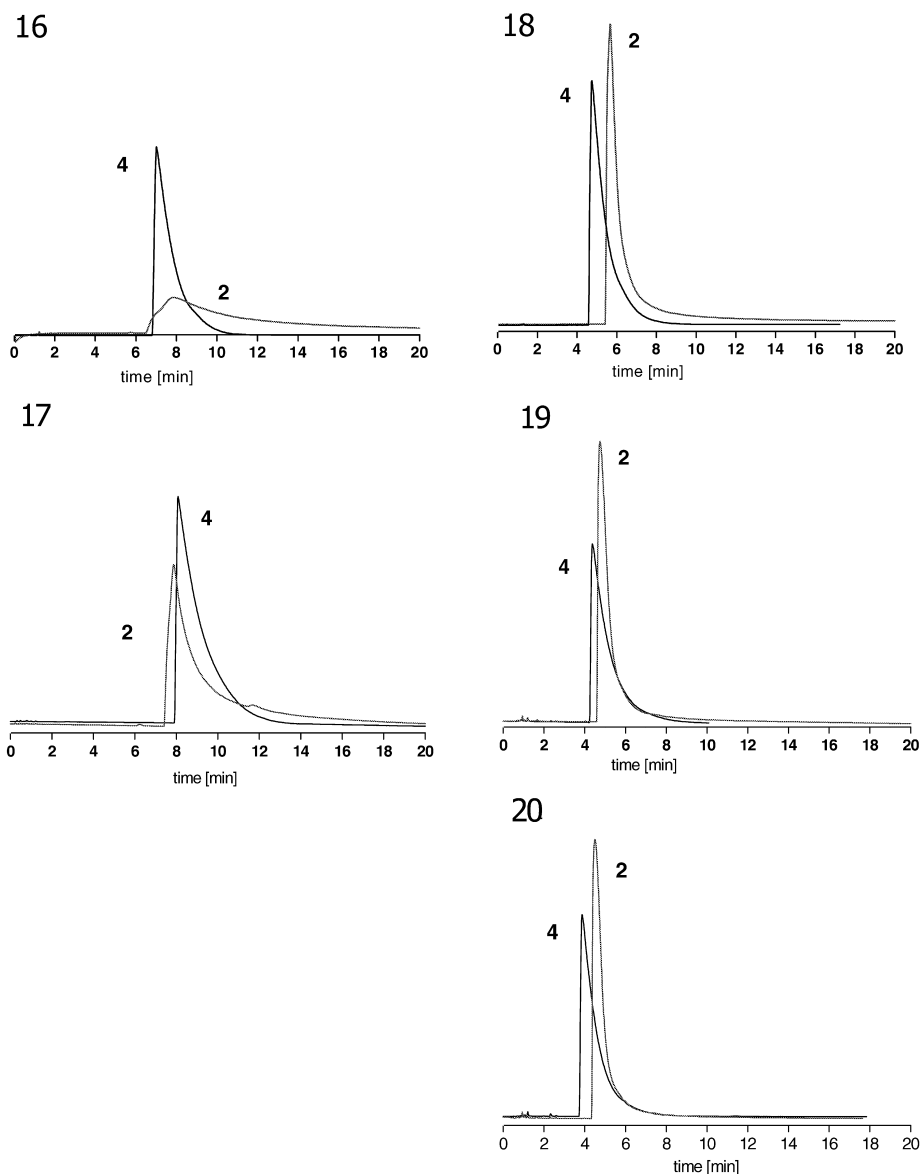


Fig. 7. Chromatograms 16–20: chromatograms of RP-18 silica Nos. 16–20. Solutes: 2,2'- (2) and 4,4'-bipyridine (4); eluent: water-methanol (51:49, v/v), column temperature 40°C, flow 1.0 ml/min, detection at 254 nm.

both isomers are therefore not only determined by the metal concentration of the parent silica. Higher bonding density of the silica (No. 19) improved the elution of both isomers compared to the lower bonded silicas (No. 17), but does not have the same efficiency as lower bonding together with endcapping of the parent silica. A good elution of both

isomers, as observed for commercial columns, was obtained for a parent silica which was treated with a dilute  $\text{Ca}(\text{OH})_2$  solution at pH 9 (Table 8). As was observed for test mixture 2, this alkaline treatment and deposition of  $\text{Ca}^{2+}$  ions on the silica surface improved the chromatographic behaviour of the metal complexing solute 2,2'-bipyridine and reduced

Table 7

Parameters for RP silica Nos. 16–20 – HCl treatment and endcapping of parent silicas, total ligand density  $\alpha_{\text{exp}}$  and elution order of 2,2'-(2) and 4,4'-bipyridine (4)

No.	Silica	HCl treatment	Endcapping	$\alpha_{\text{exp}}$ ( $\mu\text{mol}/\text{m}^2$ )	Order of elution
16	KGS1	–	–	2.65	Coelution
17	KGS3	20 h HCl	–	2.69	2, 4
18	KGS5	20 h HCl	Of KGS3	3.05	4, 2
19	KGS7	20 h HCl	–	3.12	4, 2
20	KGS8	20 h HCl	Of KGS7	3.22	4, 2

Table 8

Treatment of silica Nos. 21 and 22 – ligand density and observed elution order of 2,2'-(2) and 4,4'-bipyridine (4)

No.	Silica	Treatment	Endcapping	$\alpha_{\text{exp}}$ ( $\mu\text{mol}/\text{m}^2$ )	Elution order
21	KGS9	20 h HCl	–	3.09	4, 2
		Ca(OH) <sub>2</sub> , pH 7			
22	KGS10	20 h HCl	–	3.22	4, 2
		Ca(OH) <sub>2</sub> , pH 9			

furthermore the surface heterogeneity and surface acidity as expressed by the silanophilic tracer molecule 4,4'-bipyridine (Fig. 8).

#### 4. Conclusion

Metal contamination of size-classified silica beads could be diminished by treatment with conc. hydrochloric acid. The calcination process showed a decrease in the pore structural parameters. Sintering of the material is observed at temperatures above 700°C. Combination of dehydroxylation and rehydroxylation processes allowed the adjustment of the

surface area, the pore volume and the silanol group concentration. No dependence between the post-treatment and the ligand density/carbon content could be detected. Endcapping with HMDS also had no effect on the ligand density of the silica prepared with imidazole.

The modified silicas were tested in chromatography using the test mixtures 1, 2 and 3. Treatment of the silica with hydrochloric acid prior to silanization improved the peak symmetry of *p*-ethylaniline, pyridine together with its retention factor and 2,2'-bipyridine. No effect on the ability of separating aniline and phenol and the peak shape of 4,4'-bipyridine by this treatment was observed.

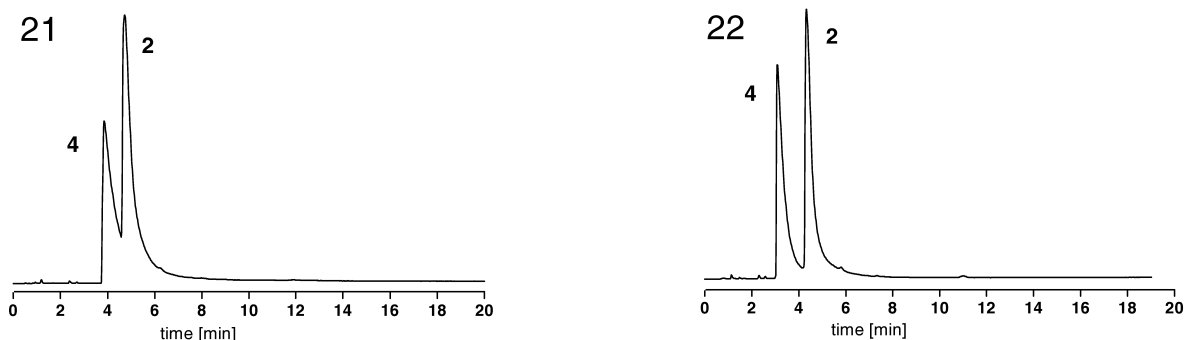


Fig. 8. Chromatograms 21 and 22: chromatograms of silica Nos. 21 and 22. Solutes: 2,2'-(2) and 4,4'-bipyridine (4); eluent: water–methanol (51:49, v/v), column temperature 40°C, flow 1.0 ml/min, detection at 254 nm.

Endcapping influenced the separation of aniline and phenol, the elution order of pyridine and phenol together with its peak symmetry and improved the retention factors and peak shapes of both isomers. Treatment of the native silicas with diluted  $\text{Ca}(\text{OH})_2$  solution improved in all cases the chromatographic behaviour.

### Acknowledgements

The authors gratefully acknowledge the financial support of the European Commission (SMT4-CT95-2026) and the Fond der Chemischen Industrie (Frankfurt/Main).

### References

- [1] K.K. Unger, F. Großmann, V. Ehwald, in: N. Tanaka, K.K. Unger (Eds.), *Reversed-Phase High-Performance Liquid Chromatography*, Elsevier, Amsterdam, in press.
- [2] H. Engelhardt, M. Arangio, *LC–GC Int.* 10 (1997) 803.
- [3] K. Kimata, K. Iwaguchi, S. Onishi, K. Jinno, R. Eksteen, K. Horosava, M. Araki, N. Tanaka, *J. Chromatogr. Sci.* 27 (1989) 721.
- [4] L.C. Sander, S.A. Wise, in: J.C. Giddings (Ed.), *Advanced Chromatography*, Marcel Dekker, New York, 1986, p. 139.
- [5] K.D. Lork, K.K. Unger, J.N. Kinkel, *J. Chromatogr.* 352 (1986) 199.
- [6] K.K. Unger, K.D. Lork, *J. Chromatogr.* 556 (1991) 395.
- [7] M. Verzele, C. Dewaele, *Chromatographia* 18 (1984) 84.
- [8] M. Mauss, H. Engelhardt, *J. Chromatogr.* 371 (1986) 235.
- [9] K.K. Unger, J. Schick-Kalib, K.F. Krebs, *J. Chromatogr.* 83 (1973) 5.
- [10] M. Holik, B. Matějková, *J. Chromatogr.* 213 (1981) 33.
- [11] F. Großmann, Ph.D. Thesis, Johannes Gutenberg-Universität, Mainz, 1998.
- [12] C. du Fresne von Hohenesche, Diploma Thesis, Johannes Gutenberg-University, Mainz, 1999.
- [13] B. Buszewski, *Chromatographia* 28 (1989) 574.
- [14] H. Engelhardt, T. Lobert, *Anal. Chem.* 71 (1999) 1885.
- [15] H. Engelhardt, *LC–GC* 15 (1997).
- [16] L.R. Snyder, in: E. Heftmann (Ed.), *Chromatography*, Part A, 5th ed., Elsevier, Amsterdam, 1992, p. 8, Chapter 1.
- [17] D.M. McCalley, *J. Chromatogr. A* 738 (1996) 169.
- [18] D. Sykora, E. Tesarova, M. Popl, *J. Chromatogr. A* 758 (1997) 37.
- [19] T. Lobert, Dissertation, Universität Saarbrücken, Saarbrücken, 1998.
- [20] W. Eymann, *Chromatographia* 45 (1997) 235.
- [21] K.K. Unger, *Porous Silica*, Elsevier, Amsterdam, 1979.
- [22] E.F. Vansant, P. Van Der Voort, K.C. Vrancken, *Studies in Surface Science and Catalysis*, Vol. 93, Elsevier, 1995.
- [23] G.E. Maciel, D.W. Sindorf, *J. Am. Chem. Soc.* 102 (1980) 7607.
- [24] L.T. Zhuravlev, *Pure Appl. Chem.* 61 (1989) 1969.
- [25] S. Kondo, H. Fujiwara, M. Muroya, *J. Colloid Interface Sci.* 55 (1976) 421.
- [26] J. Köhler, J.J. Kirkland, *J. Chromatogr.* 385 (1987) 125.
- [27] C.J. Brinker, *Sol–Gel Science*, Academic Press, 1990.
- [28] J.N. Kinkel, K.K. Unger, *J. Chromatogr.* 316 (1984) 193.
- [29] J. Nawrocki, B. Buszewski, *J. Chromatogr.* 449 (1988) 1.